Transition from ferromagnetism to superparamagnetism on the nanosecond time scale

L. Lopez-Diaz* and L. Torres
Departamento de Fisica Aplicada, Universidad de Salamanca, Salamanca E-37071, Spain

E. Moro
Theoretical Physics, University of Oxford, 1 Keble Road, Oxford OX1 3NP, United Kingdom
(Received 4 October 2001; revised manuscript received 12 March 2002; published 22 May 2002)

Langevin dynamics has been used to study different aspects of the transition from ferromagnetism to superparamagnetism when reducing the size of thin magnetic single-domain nanoparticles with in-plane uniaxial anisotropy for observation times in the order of a few nanoseconds. It is found that nonuniformities in the magnetization, usually ignored for such small particles, favor thermal relaxation. Quantitatively, the size range over which the transition occurs is found to move roughly 1 nm towards larger sizes due to this contribution. On the other hand, we also find that the thickness-dependent perpendicular demagnetizing field induces thermal switching between the two in-plane energy minima. The results are in good agreement with the Arrhenius law, which is used to characterize this effect. A strong dependence of the preexponential factor τ_0 on the particle thickness is found.

DOI: 10.1103/PhysRevB.65.224406 PACS number(s): 75.75.+a, 75.20.−g, 75.40.Mg

I. INTRODUCTION

Small ferromagnetic particles present, in general, several magnetization equilibrium states separated by energy barriers. Their hysteresis properties are the result of the evolution of the magnetization in a multistable energy landscape as a response to a varying external field. In particular, magnetic memory is based on the fact that the system remains trapped at a given metastable state over a time period much longer than the observation time t_{exp}. However, at a given temperature $T \neq 0$ thermal activation over the energy barriers leads the system towards thermodynamic equilibrium. This process is known as thermal relaxation and there is a characteristic time for it called relaxation time t_{rel}.[1] Thus, ferromagnetic hysteretic behavior is found when $t_{exp} \ll t_{rel}$, whereas in the opposite situation ($t_{exp} \gg t_{rel}$) the particle maintains the statistical equilibrium distribution of magnetization orientations as in a classical paramagnetic material. This behavior is known as superparamagnetism because the total magnetic moment of the particle is much larger than typical individual magnetic moments at atomic level. In the intermediate situation ($t_{exp} \sim t_{rel}$) nonequlibrium phenomena and magnetic relaxation occur.

In most of the literature thermal relaxation of magnetic nanoparticles is explained in terms of the Arrhenius formula

$$t_{rel} = \tau_0 \exp\left(\frac{E_B}{k_B T}\right), \tag{1}$$

where E_B is the height of the energy barrier, k_B is the Boltzmann's constant, T is the temperature, and τ_0 is a characteristic time constant, which is known to be in the range $\tau_0 \sim 10^{-10}$–10^{-12} s for magnetic nanoparticles. It is often assumed that the transition from ferromagnetism to superparamagnetism occurs when the energy barrier E_B is around $25\, k_B T$,[2] since this value gives, according to Eq. (1) and for typical values of τ_0, relaxation times of some seconds, which is in the order of t_{exp} for standard magnetic measurements. However, the growing importance of high-speed magnetoelectronics makes it necessary to understand magnetization dynamics and thermal relaxation on much shorter time scales. As an example, thermally assisted magnetization reversal in the nanosecond regime has been investigated experimentally on submicron-sized magnetic thin films.[3] In this paper we study thermal relaxation for observation times in the order of a nanosecond ($t_{exp} \sim 10^{-9}$ s). In particular, we investigate the transition from superparamagnetism to ferromagnetism as the particle size decreases. On this time scale the transition will occur for a value of $E_B/k_B T$ much smaller than 25 (for instance, $t_{exp} \sim t_{rel} = 10\,\tau_0$ gives $E_B/k_B T = \ln 10 = 2.3$). Consequently, the Arrhenius model (1), which is only valid in the high-energy barrier case ($E_B/k_B T \gg 1$),[2] is not applicable. Fortunately, there is a significant amount of research on thermal relaxation in single-domain particles that is not restricted to the high-energy barrier case. In most cases, the starting point is the Fokker-Planck equation for the system, which is the equation for the dynamics of the probability distribution of the magnetization.[4] Some techniques have been developed to solve this equation directly,[5] whereas others are based on the numerical evaluation of the eigenvalues and amplitudes of the relevant dynamical modes.[6] Both approaches give insightful information on the thermal relaxation of the particles but, due to the complexity of the Fokker-Planck equation, they are limited to problems with very few degrees of freedom and a very simple Hamiltonian. In particular, it is assumed that the magnetization of the particle is uniform and therefore, its magnetic state is specified by a single vector $\vec{M}$ and the energy of the system is given by

$$E = [\omega(\vec{M}) + \vec{M} \cdot \vec{H}_{ext}] V, \tag{2}$$

where $\omega(\vec{M})$ is the anisotropy energy density, $\vec{H}_{ext}$ is the external field, and V is the particle volume. However, exchange forces between neighboring spins are finite and $\vec{M}$ is never completely uniform inside the particle. In this work we

have investigated the effect of the small nonuniformities of $\vec{M}$ in the thermal relaxation properties of the particle. The uniform magnetization approach (from now on referred to as the *uniform-magnetization model*) is assumed to be a good approximation on the grounds that the deviations from uniform $\vec{M}$ are necessarily small in a particle of a few nm in size. Our goal is to estimate to what extent the uniform-magnetization model is a good approximation. In order to carry out our task, we have used the micromagnetic formalism, which considers the magnetization inside the particle as a continuous function of the position $\vec{M}(\vec{r})$ and, consequently, takes into account the nonuniformities in a natural way. Our approach is based on the Langevin equation, which is the Landau-Lifshitz dynamic equation for the magnetization augmented by a stochastic term that couples the system to a thermal bath.[4] This way we generate individual trajectories by numerically solving the Langevin equation and calculate the thermal relaxation properties by computing some relevant averaged quantities. Garcia-Palacios and Lazaro[7] studied some aspects of the Langevin dynamics for noninteracting magnetic nanoparticles in nonequilibrium regime ($t_{exp} \sim t_{rel}$) using the uniform-magnetization model. Langevin dynamics in the context of the micromagnetic formalism has received a lot of attention lately,[8–12] although the focus has been on particles of significantly larger size than the ones considered here, therefore presenting nonuniform switching modes[9,10] and even multidomain magnetization configurations.[11,12]

According to the Arrhenius formula (1), thermal relaxation is governed by the height of the energy barrier in the exponential, whereas the other details of the energy landscape are assumed to play a minor role and are grouped in the preexponential factor τ_0. However, these details can influence the relaxation time to a great extent, as has been pointed out by Coffey *et al.* by studying oblique applied fields and nonaxially symmetric Hamiltonians.[13,14] On the other hand, the Arrhenius model also neglects the peculiarities in the dynamics of the system under study. In particular, the precessional term in the Landau-Lifshitz equation gives rise to interesting phenomena, such as multiple crossing of the potential barrier, which are not taken into account in Eq. (1).[7] Recent studies have shown how this term influences the superparamagnetic relaxation time.[15] In particular, Palacios and Svendlindh[16] observed a field-induced interplay between precessional motion and thermoactivation that largely influences the nonlinear response of the particle. In this work we insist on these ideas, but from a different point of view. We will study thermal relaxation of a thin nanosized particle with in-plane uniaxial anisotropy and we will investigate the effect of the particle thickness on the relaxation time. We will show how the thickness-dependent perpendicular demagnetizing fields influences thermal activation over the energy barrier between the two in-plane equilibrium states.

The rest of the paper is organized as follows. In Sec. II we discuss the main features of the uniform-magnetization and micromagnetic models, as well as some details in the numerical integration of the equations. In Sec. III we present the results and discuss them. The section is divided into two parts. The first one (Sec. III A) deals with the effect of nonuniformities in $\vec{M}$, whereas the second one (Sec. III B) is focused on the role of the particle thickness. The most relevant conclusions of this work are presented in Sec. IV.

II. MODELS AND NUMERICAL TECHNIQUES

In the uniform-magnetization model, the nanoparticle is assumed to have uniform magnetization. Therefore, its magnetic state is determined by the direction of the magnetization vector $\vec{M}$ and its total magnetic moment is $\vec{M}V$. The energy of the particle in a given state is $E(\vec{M})$ and the effective field acting on $\vec{M}$ it is given by

$$\vec{H} = -\frac{1}{V}\frac{\partial E(\vec{M})}{\partial \vec{M}}, \tag{3}$$

where V is the particle volume. At $T=0$, the dynamics of the particle is given by the deterministic Landau-Lifshitz equation

$$\frac{d\vec{M}}{dt} = \gamma \vec{M}\times\vec{H} + \gamma\lambda\frac{\vec{M}}{M_s}\times(\vec{M}\times\vec{H}), \tag{4}$$

where $\gamma = -1.76\times 10^7$ Oe^{-1} s^{-1} is the gyromagnetic ratio and λ is the adimensional damping constant. Since the modulus of $\vec{M}$ is constant (its value is given by the magnetization saturation M_s) it is useful to describe the state of the particle by the adimensional unitary vector $\vec{m} = \vec{M}/M_s$. Similarly, we define the dimensionless field $\vec{h} = \vec{H}/M_s$. By multiplying Eq. (4) by $(M_s^2|\gamma|)^{-1}$ we obtain

$$\frac{d\vec{m}}{d\tau} = -\vec{m}\times\vec{h} - \lambda\vec{m}\times(\vec{m}\times\vec{h}), \tag{5}$$

where $\tau = M_s|\gamma|t$ is a dimensionless time. In order to take into account thermal agitation at $T\neq 0$, we introduce a random fluctuating field $\vec{H}_{fl}$ whose origin lies on the interaction of the magnetization with the surrounding medium (phonons, conducting electrons, nuclear spins, etc). The deterministic dynamic equation (5) is then converted into the stochastic Langevin equation

$$\frac{d\vec{m}}{d\tau} = -\vec{m}\times(\vec{h}+\vec{h}_{fl}) - \lambda\vec{m}\times(\vec{m}\times\vec{h}), \tag{6}$$

where $\vec{h}_{fl} = \vec{H}_{fl}/M_s$. It is assumed that $\vec{h}_{fl}$ is a Gaussian stochastic process whose statistical properties are given by

$$\langle h_{fl,k}(\tau)\rangle = 0, \tag{7a}$$

$$\langle h_{fl,k}(\tau)h_{fl,l}(\tau')\rangle = 2\,D\,\delta_{kl}\,\delta(\tau-\tau'), \tag{7b}$$

where k,l represent the cartesian coordinates x,y,z. Therefore, the three components of $\vec{h}_{fl}$ are independent Gaussian-distributed zero-mean white-noise terms. The constant D measures the strength of the fluctuating term. In order to determine this constant we need to construct the Fokker-Planck equation for the probability distribution of the mag-

netization $P(t)$. Because the stochastic term in Eq. (6) enters in a multiplicative way the equation must be supplemented by an interpretation in order to properly define it.[4] In this work we will follow the Stratonovich interpretation.[4] When interpreted in the Stratonovich sense, Eq. (6) yields the following Fokker-Planck equation.[17,18]

$$\frac{\partial P}{\partial \tau} = -\frac{\partial}{\partial \vec{m}} \cdot \left[-\vec{m} \times \vec{h} - \lambda \vec{m} \times (\vec{m} \times \vec{h}) + D\vec{m} \times \left(\vec{m} \times \frac{\partial}{\partial \vec{m}} \right) \right] P. \tag{8}$$

In order to ensure that the stationary properties of the system, derived from the Langevin equation (6) coincide with the correct thermal equilibrium properties, the Fokker-Planck equation (8) is forced to have the Boltzmann distribution $P_{eq}(\vec{m}) \propto \exp[-E(\vec{m})/k_B T]$ as stationary solution. This completely determines the strength of the fluctuating term

$$D = \lambda \frac{k_B T}{M_s^2 V} \tag{9}$$

as can be easily checked using Eq. (3). It should be noted that in Eq. (6) we introduced the fluctuating term only in the precessional term. Alternatively, we could have added in the damping term too. It can be shown[18] that, in that case, the Fokker-Planck equation (8) is still valid, whereas a different value for the amplitude of the noise $D = (\lambda/1 + \lambda^2) k_B T / M_s^2 V$ must be considered. Although the individual stochastic trajectories generated in both cases are different, the average properties derived from them are the same.[18]

In this paper, the Langevin equation (6) is solved numerically using a first-order Euler scheme,

$$\vec{m}(\tau + \Delta\tau) = \vec{m}(\tau) + [-\vec{m} \times \vec{h} - \lambda \vec{m} \times (\vec{m} \times \vec{h}) + 2\, D\, \vec{m}] \Delta\tau - \vec{m} \times \Delta \vec{W}, \tag{10}$$

where the three independent components of $\Delta \vec{W} = \int_{\tau}^{\tau + \Delta\tau} \vec{h}_{fl}(\tau')\, d\tau'$ are Gaussian random numbers whose statistical properties are given by

$$\langle \Delta W_k \rangle = 0, \quad \langle \Delta W_k \Delta W_l \rangle = 2\, D\, \Delta\tau\, \delta_{kl}. \tag{11}$$

The noise-induced drift term $2D\vec{m}$ has been introduced in order to have a properly defined first-order Euler scheme in the context of Stratonovich calculus.[18]

As we mentioned in Introduction, using the micromagnetic formalism we allow for the possibility of nonuniform magnetization inside the particle. In this context, Eqs. (3)–(5) are still valid if we keep in mind that $\vec{M}(\vec{r})$ and $\vec{H}(\vec{r})$ are no longer single variables but continuous functions of the position and that ordinary derivatives with respect to the magnetization become functional derivatives. Besides, a new term needs to be added to the energy functional $E(\vec{M})$ in order to take into account for the exchange interaction between the spins. On a continuous approximation, this term takes the form[2]

$$E_{exch} = \int_v A(|\nabla m_x|^2 + |\nabla m_y|^2 + |\nabla m_z|^2)\, dv, \tag{12}$$

where A is the exchange constant. The analytical expression for the other interaction terms (magnetocrystalline anisotropy E_{anis}, magnetostatic E_{demag} and external field E_{zeeman}) are trivially obtained from the ones of the uniform-magnetization model.

$$E_{anis} = \int_v \omega(\vec{m})\, dv, \tag{13}$$

$$E_{demag} = -\frac{1}{2} M_s \int_v \vec{m}(\vec{r}) \cdot \vec{H}_d(\vec{r})\, dv, \tag{14}$$

$$E_{zeeman} = -M_s \int_v \vec{m}(\vec{r}) \cdot \vec{H}_{ext}\, dv. \tag{15}$$

In the uniform-magnetization model, the demagnetizing field is given by $H_{d,i} = \Sigma_j N_{ij} M_j$, where N_{ij} are the coefficients of the self-demagnetizing tensor.[19] This leads to a quadratic shape-anisotropy term that can be absorbed into the anisotropy term $\omega(\vec{M})$.[2] In the micromagnetic model the situation is more complicated because $\vec{H}_d(\vec{r})$ is nonlocal and needs to be evaluated by solving Maxwell's equations $\nabla \cdot \vec{H}_d = -\nabla \cdot \vec{M}$ and $\nabla \times \vec{H}_d = 0$.

Although the micromagnetic continuous formalism is well established for $T = 0$, to our knowledge a model for the stochastic Langevin dynamics in this context has not been developed yet. However, in order to solve micromagnetic problems numerically the computational region is discretized and consequently, the continuous problem is converted into a problem with a finite degrees of freedom. Thus, one needs to solve a set of N equations like Eq. (6) (N being the number of mesh nodes), one for each node in the mesh. The equations are coupled between them via the effective field (the exchange and magnetostatic terms are nonlocal). Formally, this problem is analogous to that of a set of interacting uniform-magnetization particles. Consequently, the stochastic formalism described above is applicable once the spatial discretization is done. A Langevin equation (6) needs to be solved for each node in the mesh. The statistical properties of the fluctuating terms on each node $\vec{h}_{fl,\alpha}$ ($\alpha = 1,2,\ldots,N$) are given by Eqs. (7b) and (9), where now V is the volume of the computational cell. These fluctuating fields are considered to be independent of each other. In order words, we are assuming that the space correlation of the thermal noise is much smaller than the size of our computational cell. In this paper the nanoparticle is discretized in a two-dimensional square lattice of 1×1 nm cells. Equation (10) is solved on each node. The four-neighbor dot product representation is considered when discretizing the exchange term[20] whereas the demagnetizing field is calculated assuming that $\vec{m}$ is constant on each cell.

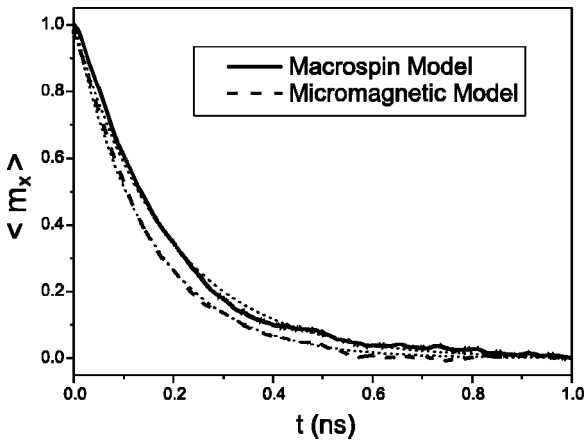

FIG. 1. Thermal relaxation of a particle with dimensions $8\times4\times1$ nm computed using the uniform-magnetization (solid line) and micromagnetic (dashed line) models. The component of the normalized magnetization along the easy axis (m_x), averaged over 7000 realizations, is plotted as a function of time (average trial invariances 2.5×19^{-4} and 2.8×19^{-4} are obtained for the uniform-magnetization and micromagnetic models, respectively). The dotted lines correspond to the exponential fit of the computed curves.

III. RESULTS AND DISCUSSION

A. Effect of nonuniformities in $\vec{M}(\vec{r})$

We consider a thin rectangular ferromagnetic particle of dimensions $8\times4\times1$ nm. The following intrinsic parameters have been used: $A=3.0\times10^{-6}$ erg/cm, $M_s=1424$ emu/cm^3, $K=0$, and $\lambda=0.1$. We note that, although these are reasonable values for ordinary ferromagnetic materials, they do not correspond to a particular one. At $T=300$ K, without applying any external field and starting with the magnetization along the positive X direction, which coincides with the easy axis, thermal relaxation is studied by monitoring the average component of the magnetization along the easy axis m_x over a large number of realizations. A fixed interval $\Delta\tau=5.0\times10^{-6}$ ($\Delta t=2.0\times10^{-16}$ s) is used in the numerical integration of the Langevin equation. Figure 1 shows the computed curves for the uniform-magnetization (solid line) and micromagnetic (dashed line) models. Both curves present the same features. The particle, initially at one of the two energy minima ($\langle m_x\rangle\simeq1$), evolves exponentially towards statistical equilibrium. Since the two equilibrium states correspond to opposite values of m_x and they both have the same energy, in statistical equilibrium they will be equally populated and consequently, $\langle m_x\rangle=0$ as $t\to\infty$. By comparing both curves we note that the relaxation is faster in the micromagnetic model. This effect can only be due to nonuniformities in $\vec{M}(\vec{r})$ inside the particle since that is the only difference between the two models. In order to make this result quantitative we consider a simple model in which the particle can only be found in one of the two equilibrium states, labeled as $(+)$ and $(-)$, with probabilities P_+ and P_-, respectively ($P_-=1-P_+$). P_+ obeys the master equation

$$\frac{dP_+}{dt}=\omega_-P_--\omega_+P_+, \tag{16}$$

where ω_+ and ω_- are the probabilities per unit time to jump from $(+)$ to $(-)$ and from $(-)$ to $(+)$, respectively. The solution of Eq. (16) is

$$P_+(t)=P_{+,eq}+[P_+(0)-P_{+,eq}]\exp\left(-\frac{t}{t_{rel}}\right), \tag{17}$$

where $P_{+,eq}$ and $P_+(0)$ are the probabilities per unit time of state $(+)$ in equilibrium and at $t=0$, respectively and t_{rel} is the relaxation time defined by $t_{rel}^{-1}=\omega_++\omega_-$. The statistical average value of m_x will be given by

$$\langle m_x(t)\rangle=m_x^{(+)}P_+(t)+m_x^{(-)}P_-(t), \tag{18}$$

where $m_x^{(+)}$ ($m_x^{(-)}$) is the value of m_x in state $(+)$ [$(-)$]. In our case we have $\omega_+=\omega_-=\omega=(2t_{rel})^{-1}$, $P_+(0)=1$, $P_{+,eq}=1/2$, $m_x^{(+)}=1$, $m_x^{(-)}=-1$. Substituting these values in Eqs. (17) and (18) we obtain

$$\langle m_x(t)\rangle=e^{-t/t_{rel}}, \tag{19}$$

which predicts an exponential decay towards statistical equilibrium. By fitting the computed curves in Fig. 1 we get $t_{rel}=1.87\times10^{-10}$ s for the uniform-magnetization model and $t_{rel}=1.50\times10^{-10}$ s for the micromagnetic model. The exponential fits are also shown in Fig. 1 (dotted lines). The discrepancies between the computed and fitted curves are attributed to two reasons. First, the two-level model we have just described is only valid in the *high-barrier* (or *low-T*) regime ($E_B/k_BT\gg1$), which is not true in our case ($E_B/k_BT\simeq1.01$). Second, this model does not take into account the dynamics given by the Landau-Lifshitz equation.

As mentioned in Introduction, we are interested in studying the transition from ferromagnetic to superparamagnetic behavior as the particle size decreases. Particles of dimensions $(L_x,L_y,L_z)=(2\,d,d,h)$ and with the intrinsic parameters given in the first paragraph of the section are considered. We have studied the stochastic dynamics at $T=300$ K during a time interval of $t_{exp}=2$ ns for different values of d keeping $h=1$ nm fixed using the uniform-magnetization model. Figure 2 shows typical individual trajectories for (a) $d=18$ nm, (b) $d=9$ nm, and (c) $d=4$ nm. The $d=18$ nm particle [Fig. 2(a)] remains in the proximity of the initial state and, therefore, is ferromagnetic on this time scale. On the contrary, the $d=4$ nm particle [Fig. 2(c)] is clearly superparamagnetic because it is continuously switching between the two energy minima. In the $d=9$ nm case [Fig. 2(b)] the characteristic switching time of the particle is of the same order than the measure time $t_{exp}=2$ ns and just a few transitions occur. In order to present statistically meaningful results we have computed 500 stochastic trajectories for each particle size. Figure 3(a) shows the statistical distribution of in-plane magnetization orientations (ϕ is the azimuthal angle in cylindrical coordinates) for $d=18$, 9, and 4 nm. We note that the distributions were obtained by frequency counting over the time interval t_{exp} and over the 500 realizations. What was observed in Fig. 2 is confirmed here. The $d=18$ nm particle presents a sharp distribution centered on the initial state ($\phi=0°$) indicating that it is able to retain its magnetic state on this time scale (ferromagnetic behavior).

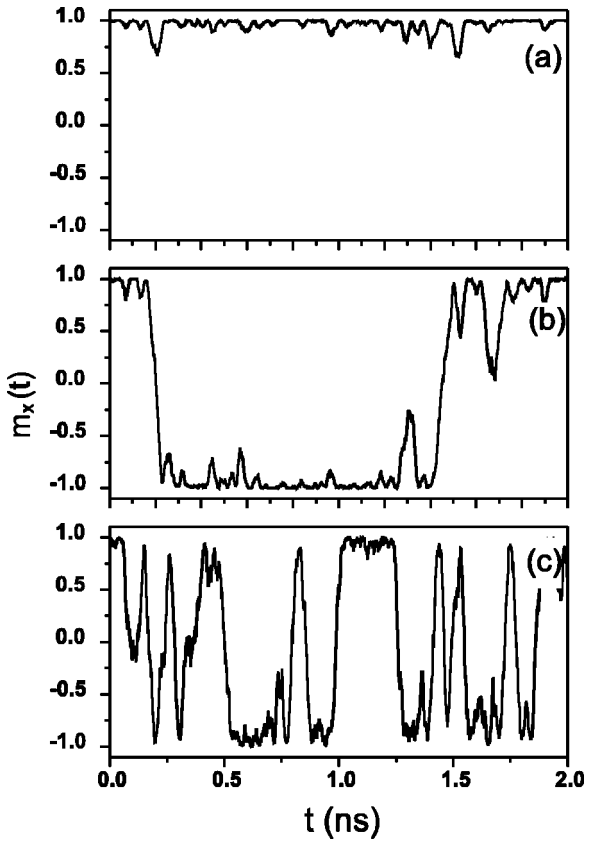

FIG. 2. Typical individual trajectories for a particle of (a) $d=18$ nm, (b) $d=9$ nm, and (c) $d=4$ nm computed using the uniform-magnetization model. The projection of $\vec{m}$ along the long axis of the particle is plotted every 2×10^{-13} s.

On the contrary, both equilibrium states are equally populated for the smallest particle, indicating that, on this time scale, the equilibrium Maxwell-Boltzman distribution is reached (superparamagnetic behavior). For the $d=9$ nm particle the magnetization has spent most of the time around $\phi=0°$, but the other peak ($\phi=180°$) is significantly populated too. The energy barrier decreases with particle size as discussed in detail below. Consequently, the low-T condition ($E_B/k_BT\gg1$) ceases to be fulfilled and the two-level description of our system is no longer valid. This can be observed by noting how the distribution around the maxima widens up as the particle size decreases.

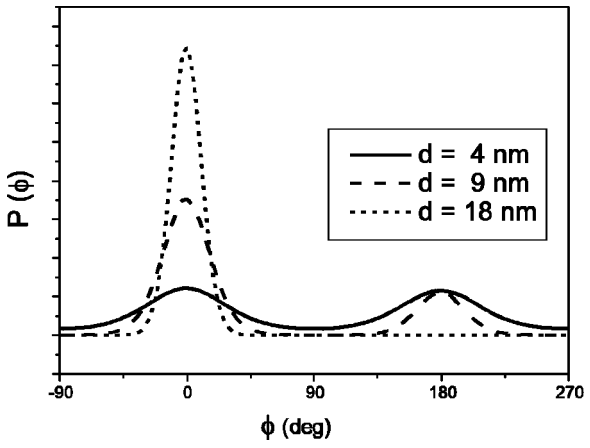

FIG. 3. Statistical distribution (over 500 trials) of in-plane orientations for three different particle sizes during a time interval $t_{exp}=2$ ns computed using the uniform magnetization model.

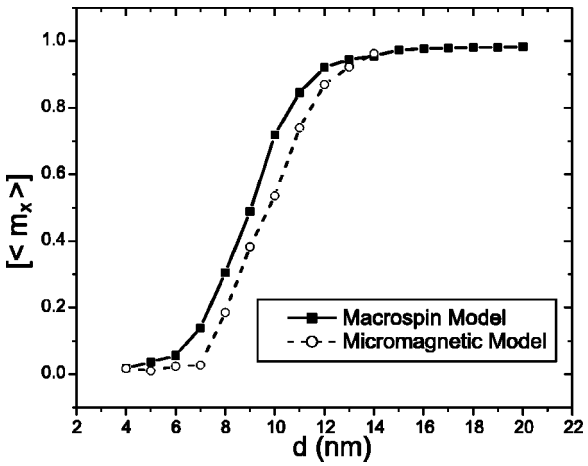

FIG. 4. Average value of m_x over the time interval $t_{exp}=2$ ns for different particle sizes computed using the uniform-magnetization and micromagnetic models.

The results presented in Figs. 2 and 3 have been obtained using the uniform-magnetization model. When using the micromagnetic model very similar results are obtained. However, quantitatively there is a small difference between the two models. In order to measure this difference, the average value of $\langle m_x\rangle$ over the time interval $t_{exp}=2$ ns has been computed. We represent this quantity by $[\langle m_x\rangle]_{t_{exp}=2\ ns}$, where

$$[\langle m_x\rangle]_{t_{exp}}=\frac{1}{t_{exp}}\int_0^{t_{exp}}\langle m_x(t)\rangle dt. \tag{20}$$

This variable would correspond to the measured value of m_x over an ensemble of non-interacting identical particles in an experiment with characteristic observation time t_{exp}. We note that $[\cdots]$ indicates average over a time interval, whereas $\langle\cdots\rangle$ indicates average over many individual Langevin realizations. In Fig. 4 we have plotted $[\langle m_x\rangle]_{t_{exp}=2\ ns}$ as a function of particle size computed using the uniform-magnetization and micromagnetic models. The larger particles ($d\geqslant14$ nm) are ferromagnetic because they retain their magnetic state over the time interval of the measurement. On the contrary, for the smallest particles ($d\leqslant6$ nm) the magnetic memory is lost. The transition between the two behaviors is gradual and takes place in a range of a few nanometers. Interestingly, this transition is slightly moved towards larger d, roughly 1 nm, when the micromagnetic model is used. These results confirm what we anticipated when discussing Fig. 1, that nonuniformities in the magnetization assist thermal switching, and it provides an estimate of the error introduced when the uniform-magnetization model is used.

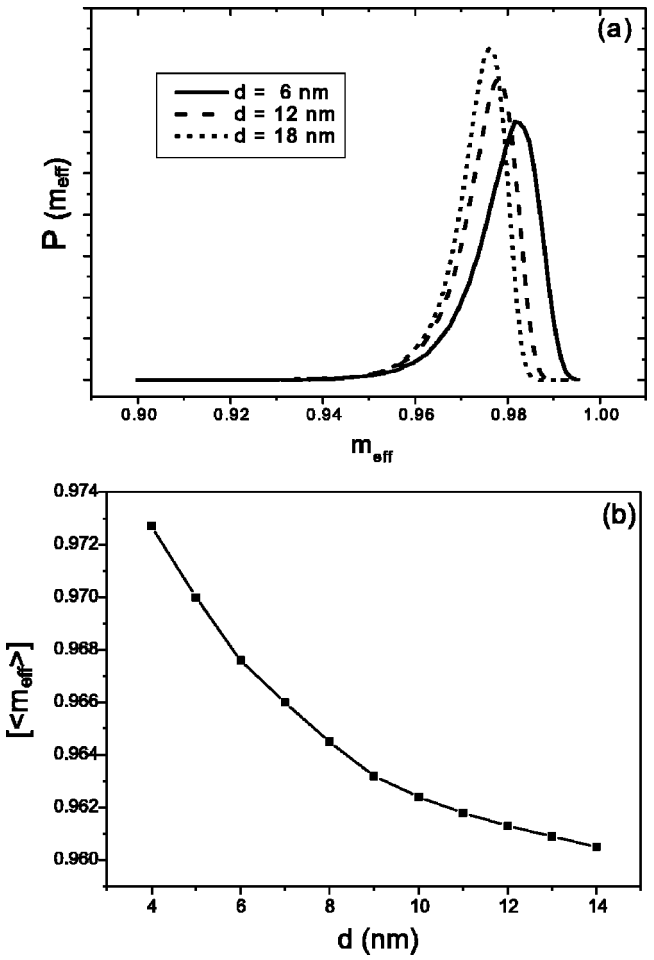

FIG. 5. (a) Statistical distribution of $m_{eff}=M_{s,eff}/M_s$ [see Eq. (21)] for three different particle sizes. (b) Time ($t_{exp}=2$ ns) and statistical (500 realizations) average value of m_{eff} as a function of particle size.

It is well known that small deviations from uniform magnetization are responsible for what is called configurational anisotropy,[21] which is well characterized for elements of regular shape and whose order and magntitude is closely connected with the symmetry of the particle. We would like to point out that the contribution analyzed here is not related to the configurational anisotropy since, as estimated in Ref. 22, this contribution is negligible below $d=40$ nm. On the other hand, it could be thought that the difference observed when using the micromagnetic model is due to the occurrence of reversal modes different from coherent rotation that cannot be accounted for in the uniform-magnetization model. A good measure of the degree of nonuniformity in a given micromagnetic configuration is provided by what we call the *effective saturation magnetization*, $M_{s,eff}$, defined by

$$M_{s,eff}=\frac{1}{V}\left\{\sum_{i=x,y,z}\left[\int_V M_i(\vec{r})dV\right]^2\right\}^{1/2}. \qquad (21)$$

When the magnetization inside the particle is perfectly aligned we have $\int_V M_i dV=M_i V$ and $M_x^2+M_y^2+M_z^2=M_s^2$, therefore $M_{s,eff}=M_s$. In any other case we have $M_{s,eff}<M_s$. Figure 5(a) shows the statistical distribution of $m_{eff}=M_{s,eff}/M_s$ for three different particle sizes over a time period $t_{exp}=2$ ns and after 500 realizations, although this distribution is observed to be independent of the time scale and on the number or realizations, provided that this last one is large enrough. Figure 5(b) shows the averaged value of m_{eff} of different particle sizes for the same time scale and number of realizations of Fig. 5(a). It is observed that the deviation from $m_{eff}=1$ increases with d as one would expect, since as the particle size increases nonuniformities in $\vec{M}$ become more energetically favorable. In any case, the average value is always very close to $m_{eff}=1$, indicating that there is almost complete alignment inside the particles. It is noticeable, however, that in Fig. 5(a) there is a conspicuous asymmetry in the statistical distribution towards lower values of m_{eff}. Although it has not been analyzed in detail, the points on the left tail of the distribution probably correspond to the situations in which the particle is switching between the two energy minima, since nonuniform configurations are more likely to occur when the particle is far from equilibrium. Nevertheless, no value below $m_{eff}<0.9$ has been found in any case, even for the largest particles simulated ($d=20$ nm), which completely rules out switching modes other than quasicoherent rotation. This is an expected result because, for a given material, the distance over which the magnetization direction changes significantly is given by the exchange length $l_{ex}=[A/(2\pi M_s^2)]^{1/2}$, which in our case has the value $l_{ex}=4.85$ nm. Since the particle sizes considered here are of the same order of magnitude, highly non-uniform states are very unfavorable energetically. On the other hand, one might wonder whether the results for the micromagnetic model would be altered in case of changing the cell size. An exhaustive study of the dependence on the cell size would require a lot of computation time and is beyond the scope of this paper. It can be anticipated, though, that a smaller cell size would favor nonuniformities in the magnetization and, consequently, the effect analyzed in this section would be amplified. However, a few particle sizes have been simulated reducing the cell size to 0.5 nm and no significant differences with respect to the results presented in Fig. 5 have been found.

It has already been mentioned that the Arrhenius formula (1) and the two-level description of the system (16) are only valid in the high-barrier regime ($E_B/K_BT\gg 1$). As will be shown below, this is not the case for the results that have been presented in this section. However, it is interesting to estimate to what extent the behavior predicted from these two approximations differ from the results based on Langevin dynamics we have just presented. According to the exponential decay law predicted by the two-level approximation, Eq. (19), we obtain the following expression for $[\langle m_x\rangle]$:

$$[\langle m_x\rangle]_{t_{exp}}=\frac{1}{t_{exp}}\int_0^{t_{exp}} e^{-t/t_{rel}}dt=\frac{t_{rel}}{t_{exp}}(1-e^{-t_{exp}/t_{rel}}), \qquad (22)$$

where the relaxation time t_{rel} is given by Eq. (1). The shape-anisotropy energy barrier is given by

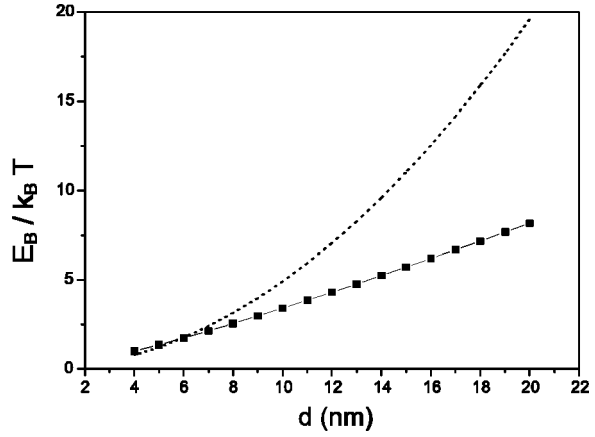

FIG. 6. Dependence of the energy barrier on particle size (solid line with square symbols). The dotted line is obtained when the dependence of the demagnetizing factors on the particle size is ignored.

$$E_B = \frac{1}{2} M_s^2 (D_y - D_x) V, \tag{23}$$

where D_x and D_y are the demagnetizing factors along the X and Y directions, respectively.[23] Since $V = 2\,d^2 h$, one could think that E_B is proportional to d^2, but the dependence is significantly weaker because the demagnetizing factors D_x and D_y (and their difference) decrease with increasing d (we are keeping h constant). Figure 6 is a plot of the energy barrier E_B/K_BT as a function of particle size (solid line with square symbols), where the analytical expressions for the demagnetizing factors of rectangular prisms obtained in Ref. 23 have been used. The curve is compared with the quadratic curve obtained when the dependence of the demagnetizing factors on d is ignored. Once the energy barrier for a given d is known, the theoretical curve given by Eqs. (22), (1), and (23) is fully determined except for the parameter τ_0. In Fig. 7 we represent the fit of the computed curves in the uniform-magnetization and micromagnetic models to the theoretical law. The values $\tau_0 = 6.24 \times 10^{-11}$ s and $\tau_0 = 4.43 \times 10^{-11}$ s were obtained for the uniform-magnetization and micromagnetic models, respectively. It can be observed that, in both cases, the computed curves predict a faster transition than the analytical approximation. The reasons for the discrepancies are attributed to the same two reasons that were outlined when discussing Fig. 1: we are not in the high-barrier regime and the three-dimensional dynamics of the magnetization is not taken into account. The following section focuses on this latter aspect.

B. Effect of particle thickness

As pointed out in Secs. I and III A, the precessional nature of magnetization dynamics in conjunction with the peculiarities of the energy landscape can play an important role in the thermal properties of nanoparticles. It is only very recently that these effects have started to be studied. In Ref. 24, Garanin *et al.* found that the time-dependent saddle point created by an oblique applied field in the anisotropy potential

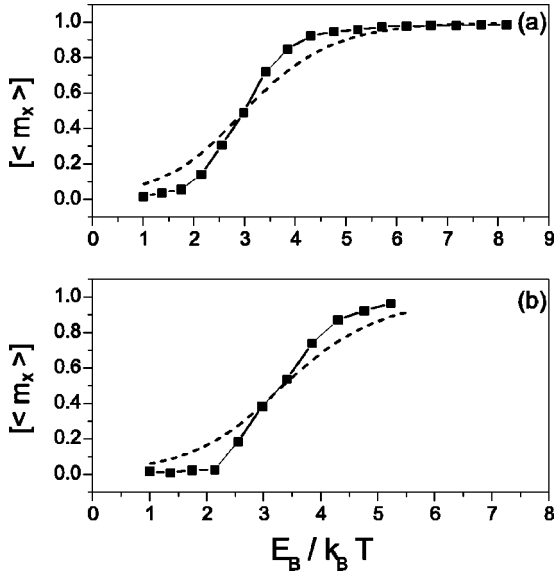

FIG. 7. Fit of the computed (a) uniform-magnetization and (b) micromagnetic curves to the theoretical law given by the two-level model [Eq. (22)] and the Arrhenius law [Eq. (1)]. The solid line with the square symbols corresponds to the computed curve, whereas the dashed line corresponds to the fit. The only parameter in the fit is τ_0.

barrier favors interpotential jumps. Here we study similar effects considering the influence of the particle thickness on the magnetization dynamics.

In this section we consider thin square nanoparticles of dimensions $d \times d \times h$ and intrinsic parameters $M_s = 1424$ emu/cm^3, $\lambda = 0.1$ and $K = 5 \times 10^5$ erg/cm^3, with the magnetocrystalline anisotropy axis (X direction) parallel to two edges of the square. Although the physical origin of the anisotropy term is different than in the previous section, we also have two equilibrium states ($m_x = \pm 1$) separated by an energy barrier. The reason for this change will become clear below. On the other hand, once the role of nonuniformities in $\vec{M}$ has been studied in the previous section, it can be anticipated that their inclusion will not lead to significant changes in the results that follow. Therefore, and in order to save computing resources, only the uniform-magnetization model has been used in this section.

As outlined before, our aim in this section is to study the effect of the thickness-induced demagnetizing field on the Langevin dynamics of thin nanoparticles. In order to do that, we first isolate this contribution by comparing thermal relaxation curves computed with and without including the demagnetizing field. When ignoring this contribution we want to preserve the two energy minima and the height of the barrier between them. This is achieved by simply ''switching off'' magnetostatic interactions, but it would not be possible in the case of having a shape anisotropy barrier, like in the previous section.

In Fig. 8, a three-dimensional plot of magnetization orientations during a time interval $t_{exp} = 4$ ns is presented both with [Fig. 8(a)] and without [Fig. 8(b)] including the demagnetizing field. The magnetic states (m_x, m_y, m_z) are plotted as points in the unit sphere ($m_x^2 + m_y^2 + m_z^2 = 1$) at a sampling

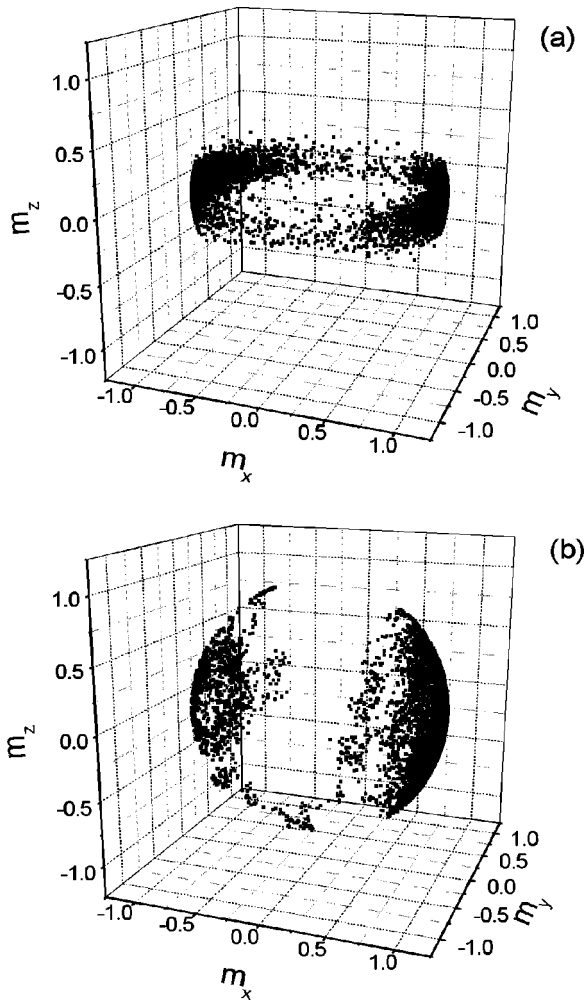

FIG. 8. Three-dimensional plot of magnetization orientations during a time interval $t_{exp}=4$ ns for a uniaxial particle of dimensions $10\times10\times1$ nm (a) with and (b) without considering the demagnetizing field. The magnetic states (m_x, m_y, m_z) are plotted as points in the unit sphere $(m_x^2+m_y^2+m_z^2=1)$ at a sampling rate of 10^{-12} s.

rate of 10^{-12} s. The particle considered has dimensions $10\times10\times1$ nm and a fixed interval $\Delta\tau=1.0\times10^{-4}$ $(\Delta t=4.0\times10^{-15}$ s) was used in the numeric integration of the Langevin equation. Due to the low thickness-to-length ratio (1:10), the magnetostatic term tends to constrain the motion of the magnetization into the X-Y plane, as can be observed by comparing Figs. 8(a) and 8(b). In principle, it could be thought that this contribution hinders thermal relaxation, since potential barrier crossings with a strong perpendicular component m_z are energetically unfavorable; therefore, constraining the possible ways of escape to those in which $\vec{M}$ is mostly contained in the plane of the particle (X-Y). However, the effect is the opposite, as shown in Fig. 9, where the time evolution of $\langle m_x\rangle$ at $T=300$ K is represented both with (solid line) and without (dashed line) the magnetostatic term. Thermal relaxation is found to be considerably faster when the demagnetizing field is taken into account. Quantitatively, by fitting the computed curves to the exponential law in Eq.

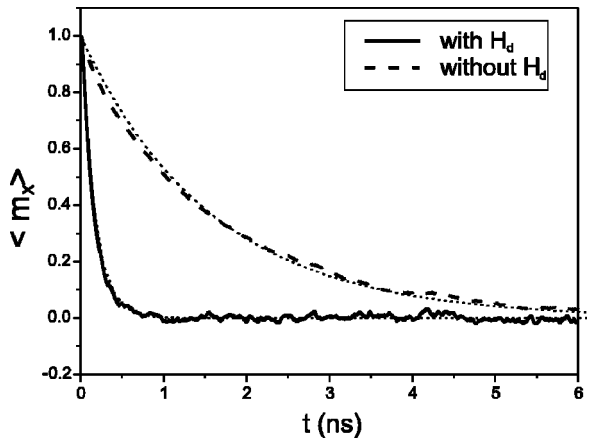

FIG. 9. Thermal relaxation of a square nanoparticle ($d=10$ nm, $h=1$ nm) with magnetocrystalline uniaxial anisotropy computed with (solid line) and without (dashed line) considering the demagnetizing field. The component of the normalized magnetization along the easy axis (m_x), averaged over 5000 realizations, is plotted as a function of time. The dotted line corresponds to the exponential fit of the computed curves.

(19), we obtain $t_{rel}=1.67\times10^{-10}$ s when including $\vec{H}_d$ and $t_{rel}=1.57\times10^{-9}$ in the other case. The theoretical fits are shown as thin dotted lines in the figure. The explanation of this effect is based on the precessional nature of magnetization dynamics, as shown schematically in Fig. 10, where the projections on the X-Y and X-Z planes of the relevant vectors for magnetization dynamics are represented. At a given time instant, let us consider the magnetization vector $\vec{M}$ in the proximity of one equilibrium state with a nonzero perpendicular component $(m_z\neq0)$, as shown in Fig. 10 (for simplicity, we have considered $m_y=0$). Due to the thinness

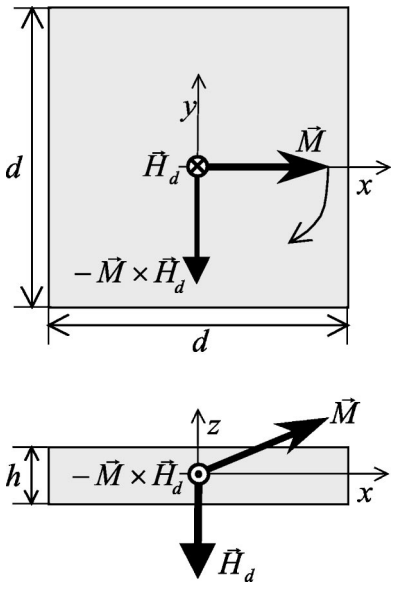

FIG. 10. Schematic representation of relevant vectors for understanding thickness-induced switching in a thin square particle. The top figure represents a projection in the X-Y plane, whereas the bottom one corresponds to the projection in the X-Z plane.

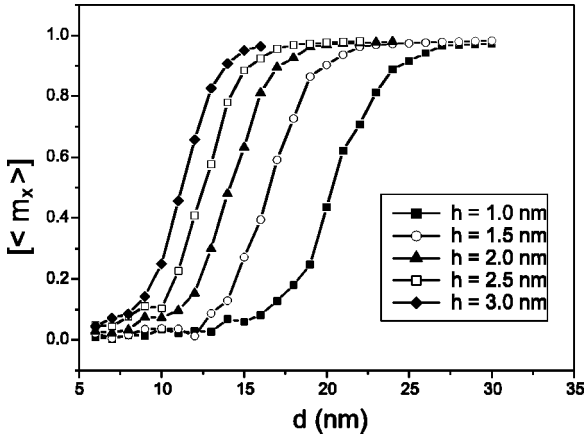

FIG. 11. Average value of m_x over the time interval $t_{exp}=8$ ns as a function of particle size d for different values of the particle thickness h.

of the particle, the perpendicular component m_z creates a strong demagnetizing field in the opposite direction (see Fig. 10). The gyromagnetic term in the Landau-Lifshitz equation (4), dominant in our case ($\lambda=0.1$), forces $\vec{M}$ to move in the direction of $-\vec{M}\times\vec{H}_d$, as indicated by the curved arrow in Fig. 10, therefore favoring switching over the energy barrier. That the precessional motion around the thickness-induced demagnetizing field favors magnetization reversal has been emphasized recently[25,26] but, to our knowledge, its effect on thermal relaxation has not been studied yet. We have computed $[\langle m_x\rangle]$ for different particle sizes and thicknesses over a time interval $t_{exp}=8$ ns and averaging over 200 realizations. The results are shown in Fig. 11. As can be observed, the transition from ferromagnetism to superparamagnetism moves towards larger particle sizes as the thickness is reduced. However, this result cannot be attributed only to the effect described above, since the height of the energy barrier, which is given by

$$E_B = K\,V = K\,d^2 t, \tag{24}$$

is different for each thickness. However, it is possible to isolate the contribution under study by fitting each curve in Fig. 11 to the theoretical law given by Eqs. (22) and (1). Figure 12(a) shows the fit corresponding to the $h=1$ nm curve. The agreement between the computed values and the theoretical curve is reasonable. A similar agreement is found in the other cases. The effect of the thickness-induced demagnetizing field is fully contained in the characteristic time τ_0, whereas the contribution due to the height of the energy barrier, which is completely determined using Eq. (24), is contained in the exponential factor $\exp(E_B/k_BT)$. In Fig. 12(b) the values of τ_0 obtained in the fitting process are plotted as a function of particle thickness. It is confirmed that a reduction in the thickness favors thermal activation due to precessional motion around the out-of-plane demagnetizing field. A strong dependence is found in the range covered (70% increase in τ_0 over a thickness range of 2 nm).

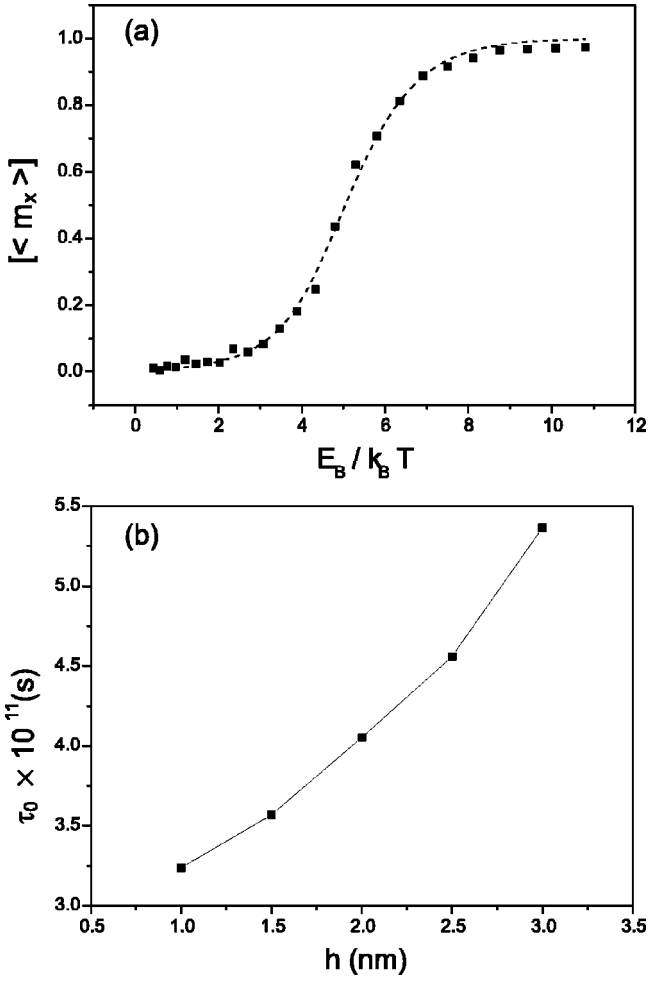

FIG. 12. (a) Fit of the computed curve for a particle with $h=1$ nm and $d=10$ nm to the theoretical law given by of Eq. (22), where t_{rel} is given by Eq. (1). (b) Plot of the values of τ_0 obtained by fitting the computed curves for different particle thicknesses.

IV. CONCLUSIONS

In this work we have studied thermal relaxation in single-domain particles with uniaxial anisotropy by using a Langevin approach. By monitoring the average value over a time interval t_{exp} of the magnetization component along the particle easy axis, the transition from ferromagnetic to superparamagnetic behavior has been characterized. Although not as powerful as the techniques based directly on the Fokker-Planck equation, the Langevin approach can handle problems that are intractable otherwise and also provides physical insight into the problem under study because it yields individual stochastic trajectories from which averaged quantities can be computed.

The first aspect we have focused on is the contribution due to nonuniformities in the magnetization. For particles of a few nanometers in size, the nonuniformities are usually ignored and the uniform-magnetization model is used. The error introduced when such an approximation is considered has been estimated. This error might be negligible in practice for the particle sizes considered here. Considering the significant increase in difficulties and computer power demands

when using the micromagnetic model, we conclude that the uniform-magnetization model is a good approximation for the time scale and particle sizes considered. However, for slightly larger particles nonuniform reversal modes occur and a micromagnetic approach becomes necessary.

Second, we have studied the effect of the thickness-induced demagnetizing field. The gradient of the energy in the plane perpendicular to the long axis of the particle plays an important role in the precessional motion of the magnetization, which significantly influences the thermal relaxation properties. The results are fitted to an analytical formula derived assuming that the relaxation time is given by the Arrhenius law and that the particle can only be in one of the two equilibrium states (two-level description). Although these assumptions are only valid in the high-barrier limit and we are in the $E_B \sim k_B T$ regime, a good agreement is found. That allowed us to characterize the effect under study by a dependence of the parameter τ_0 on the particle thickness.

ACKNOWLEDGMENTS

The authors would like to thank J. Rothman for helpful discussions. This work was partially supported by the Spanish Department of Education and Culture under project PB98-0264 and by the Government of *Castilla y Leon* under project SA 056/02.

*Electronic address: lld@usal.es

[1] W.T. Coffey, Adv. Chem. Phys. **103**, 259 (1998). There are different ways to define the relaxation time. This paper presents a comprehensive review of the different definitions.

[2] G. Bertotti, *Hysteresis in Magnetism* (Academic Press, San Diego, 1998).

[3] R.H. Koch, G. Grinstein, G.A. Keefe, Y. Lu, P.L. Trouilloud, W.J. Gallagher, and S.S.P. Parkin, Phys. Rev. Lett. **84**, 5419 (2000).

[4] N.G. van Kampen, *Stochastic Processes in Physics and Chemistry* (North-Holland, Amsterdam, 1981).

[5] D. Rodé, H.N. Bertram, and D.R. Fredkin, IEEE Trans. Magn. **MAG-23**, 2224 (1987).

[6] W.T. Coffey, D.S.F. Crothers, Y.P. Kalmykov, E.S. Massawe, and J.T. Waldron, Phys. Rev. E **49**, 1869 (1994).

[7] J.L. Garcia-Palacios and F.J. Lazaro, Phys. Rev. B **58**, 14 937 (1998).

[8] E.D. Boerner and H.N. Bertram, IEEE Trans. Magn. **33**, 3052 (1997).

[9] K.Z. Zhang and D.R. Fredkin, J. Appl. Phys. **85**, 5208 (1999).

[10] G. Brown, M.A. Novotny, and P.A. Rikvold, J. Appl. Phys. **89**, 7588 (2001).

[11] L. Lopez-Diaz, E. Della Torre, and E. Moro, J. Appl. Phys. **85**, 4367 (1999).

[12] T. Schrefl, W. Scholz, D. Suess, and J. Fidler, IEEE Trans. Magn. **36**, 3189 (2000).

[13] W.T. Coffey, D.S.F. Crothers, J.L. Dormann, L.J. Geoghegan, Y.P. Kalmykov, J.T. Waldron, and A.W. Wickstead, J. Magn. Magn. Mater. **145**, L263 (1995).

[14] W.T. Coffey, D.S.F. Crothers, J.L. Dormann, L.J. Geoghegan, and E.C. Kennedy, J. Magn. Magn. Mater. **173**, L219 (1997).

[15] W.T. Coffey, D.S.F. Crothers, J.L. Dormann, Y.P. Kalmykov, and S.V. Titov, Phys. Rev. B **64**, 012411 (2001).

[16] J.L. Garcia-Palacios and P. Svedlindh, Phys. Rev. Lett. **85**, 3724 (2000).

[17] H. Risken, *The Fokker-Planck Equation*, 2nd ed. (Springer, Berlin, 1989).

[18] J.L. Garcia-Palacios, Adv. Chem. Phys. **112**, 1 (2000).

[19] Strictly speaking, $H_{d,i} = -\Sigma_j N_{ij} M_j$ is only valid for ellipsoidal particles (in which case N_{ij} is diagonal when referred to the principal axes of the ellipsoid), since in any other case the demagnetizing field is not constant. However, the expression can be generalized to any uniformly magnetized body considering that $\vec{H}_d$ is the average demagnetizing field inside the particle. A.J. Newell, W. Williams, and D.J. Dunlop, J. Geophys. Res., [Solid Earth] **98**, 9551 (1993).

[20] M.J. Donahue and R.D. McMichael, Physica B **233**, 272 (1997).

[21] R.P. Cowburn, A.O. Adeyeye, and M.E. Welland, Phys. Rev. Lett. **81**, 5414 (1998).

[22] R.P. Cowburn, D.K. Koltsov, A.O. Adeyeye, and M.E. Welland, Europhys. Lett. **48**, 221 (1999).

[23] The self-demagnetizing tensor is diagonal for rectangular prisms: $N_{ij} = -D_i \delta_{ij}$. A. Aharoni, J. Appl. Phys. **83**, 3432 (1998).

[24] D.A. Garanin, E.C. Kennedy, D.S.F. Crothers, and W.T. Coffey, Phys. Rev. E **60**, 6499 (2000).

[25] J. Miltat and A. Thiaville, Science **290**, 466 (2000).

[26] C.H. Back, R. Allenspach, W. Weber, S.S.P. Parkin, D. Weller, E.L. Garwin, and H.C. Siegmann, Science **285**, 864 (1999).